Reprinted from

Biochimica et Biophysica Acta, 462 (1977) 622–641

BBA 47411

THE DIMERIZATION OF PROTOCHLOROPHYLL PIGMENTS IN NON-POLAR SOLVENTS

ALBERT RASQUAIN, CLAUDE HOUSSIER and CYRILLE SIRONVAL

Laboratoire de Photobiologie, Département de Botanique and Laboratoire de Chimie-Physique, Université de Liège, Sart Tilman, B4000 Liège (Belgium)

(Received May 26th, 1977)

SUMMARY

The infrared, visible and nuclear magnetic resonance spectra of protochlorophyll *a* and vinylprotochlorophyll *a* in dry non-polar solvents (carbon tetrachloride, chloroform, cyclohexane) are presented and interpreted in terms of dimer interaction.

The infrared spectra in the 1600–1800 cm^{-1} region clearly show the existence of a coordination interaction between the C-9 ketone oxygen function of one molecule and the central magnesium atom of another molecule. Infrared spectra in the OH stretching region (3200–3800 cm^{-1}) provide a valuable test of the water content in the samples.

The analysis of the absorption and circular dichroism spectra of protochlorophyll *a* and vinylprotochlorophyll *a* in carbon tetrachloride demonstrates the existence of a monomer-dimer equilibrium in the concentration range from 10^{-6} to $5 \cdot 10^{-4}$ M. The dimerization constants are $(6 \pm 2) \cdot 10^5$ $1 \cdot M^{-1}$ for protochlorophyll *a* and $(4.5 \pm 2) \cdot 10^5$ $1 \cdot M^{-1}$ for vinylprotochlorophyll *a* at 20 °C. The deconvolution of visible spectra in the red region has been performed in order to obtain quantitative information on the dimer structure. Two models involving a parallel or a perpendicular arrangement of the associated molecules are considered.

From ^1H NMR spectra, it appears that the region of overlap occurs near ring V, in agreement with the interpretation of the infrared spectra.

INTRODUCTION

It is now well established that in the etioplast, protochlorophyll(ide) molecules are associated with lipoproteins in a highly specific way. There is evidence that the way the pigments are arranged spatially is of particular interest when considering the process of photoreduction of protochlorophyll(ide) into chlorophyll(ide).

Several studies [1–6] of visible spectra of etiolated leaves or homogenates indicate that the pigment molecules are in close proximity in the etioplast. Mathis and

Abbreviations: PChl(ide), protochlorophyll(ide); PChl-*a*, protochlorophyll *a*; VPChl-*a*, vinylprotochlorophyll *a*; Chl-*a*, chlorophyll *a*; CD, circular dichroism.

Sauer [6], as well as Schultz and Sauer [5], postulated that an active PChl(ide) · lipoprotein complex molecule contains two interacting PChl(ide) molecules. This conclusion is in agreement with measurements of Schopfer and Siegelman [7] who found at least two molecules of pigment per protein of 600 000 molecular weight.

The study of the aggregation properties, in vitro, is expected to give information on the PChl(ide)-PChl(ide) interactions in vivo. From infrared [8] and circular dichroism measurements [10], Houssier and Sauer obtained argument in favour of the aggregation of protochlorophyll *a* and vinylprotochlorophyll *a* in dry carbon tetrachloride. From the observation of an "aggregated" ketone carbonyl band at 1668 cm^{-1}, they concluded that PChl-*a* molecules aggregate in a similar way to Chl-*a* molecules, i.e. through a C = O - - - Mg bond (see formula, Fig. 10). The exciton splitting of the circular dichroism bands supports this conclusion; the aggregate (probably a dimer) appears to be formed in non-polar solvents, in the absence of other nucleophile molecules such as alcohol and water molecules.

A very different aggregation behaviour has been observed for protochlorophyllide in less drastic conditions of dryness by Seliskar and Ke [11] and Brouers [12]. Spectral changes in the visible and fluorescence emission were interpreted as reflecting the formation of aggregates of high molecular weight.

Many aspects of PChl(ide) behaviour in non polar solvents are understandable by considering the aggregation properties of Chl pigments. Infrared studies [13, 14], proton magnetic resonance [15–18], visible spectroscopy [19, 20] and molecular weight [21] determinations showed that Chl-*a* forms dimers (Chl_2) in carbon tetrachloride and benzene and oligomers in hydrocarbons. It is known that the central Mg atom with a coordination number of four is unsaturated; in these cases, an electron donor group occupies at least one of the Mg axial positions (a molecule of polar solvent, water, alcohol etc . . . , or another Chl molecule via its keto function of ring V). ^{13}C nuclear magnetic resonance experiments [18] gave strong evidence for donor participation of the keto group of ring V in Chl-*a* dimerization.

The Chl-water interaction requires special comments. Large changes in the infrared [22–25], visible [23, 24, 26, 27] and circular dichroism [20] spectra have been interpreted in terms of aggregates in which molecules are linked to each other by water molecules through the intervention of a hydrogen bond.

The structural features of Chl-*a* dimers, oligomers and water adducts, in vitro, have been used as a model for the arrangement of pigment molecules in the thylakoid [28–31]. In order to obtain information on the arrangement of PChl(ide) in vivo, it is of particular interest to compare the spectral properties of PChl-*a* aggregates prepared either in the presence or in the absence of water. In this paper, we will be exclusively interested in the aggregation properties of PChl-*a* and VPChl-*a* (phytylated pigments) in dry non polar solvents (carbon tetrachloride, chloroform, benzene, cyclohexane). Rather large amounts of phytylated pigments are available in pumpkin seed coats. A procedure which yields very pure PChl-*a* and VPChl-*a* will appear elsewhere with full details (Houssier, C. and Rasquain, A., to be published). Excluding water from the solution of PChl pigments causes some difficulties; so we paid much attention to the procedures for drying pigments and solvents.

We used infrared spectroscopy as a test in order to define the best conditions of aggregation in pure dry solvents. The visible absorption and circular dichroism data were best interpreted by assuming the existence of a monomer-dimer equilibrium in

these solvents. A deconvolution of these spectra was performed in order to obtain quantitative information on the dimer structure. ^1H NMR was used to follow the formation of PChl-*a* dimer in C^2HCl_3 and to obtain additional information on the geometry of the dimer.

MATERIALS AND METHODS

Extraction and purification of protochlorophyll pigments

PChl-*a* and VPChl-*a* were prepared from pumpkin seed coats by a procedure described elsewhere (Houssier, C. and Rasquain, A., to be published). The acetone, benzene and isooctane solvents used in the preparation were reagent grade (UCB or Merck). The diethyl ether was Baker analyzed Reagent, anhydrous (peroxide content, maximum 0.00001 %) without further purification.

Preparation of solutions

Before use, PChl pigments were rechromatographed on a sugar column and thoroughly dried by the following procedure: PChl-*a* was dissolved in dry CCl_4 and the solvent removed by evaporation at room temperature in a stream of dry nitrogen. This procedure was repeated at least three times, and finally the precipitated pigment was dried under 10^{-4} mm of Hg for one week. It has been shown by Houssier and Sauer [8] that more drastic conditions of drying with heating above 40–50 °C (as for Chl-*a*) yielded altered pigments.

The solvents used for the study of aggregation (CCl_4, $CHCl_3$, C^2HCl_3, methanol, propanol, cyclohexane) were analytical reagent grade (Merck). They were dried during three days over activated molecular sieve 4 Å. The amount of water was checked by infrared spectroscopy at 1.89 μm where less than 10^{-5} M can be detected.

All stock solutions and dilutions were prepared under dry nitrogen, using flasks, pipets and cuvettes, previously dried at 100 °C under vacuum for 2 h. All manipulations of the pigment solutions were performed under yellow light to avoid photodecomposition.

Spectral measurements

The infrared spectra were measured with a Beckman IR 12 spectrophotometer equipped with an expanded scale system. We used sodium chloride and Irtran microcells (RIC). The samples were prepared by dissolving PChl-*a* in the appropriate solvent (concentration 10^{-1} to 10^{-2} M).

The absorption spectra in the visible range were recorded using a CARY 17 spectrophotometer or a JASCO ORD/UV-5 spectrophotometer equipped with a CD attachment. The instrument was calibrated with a solution of (+)-camphorsulfonic acid (1 mg/ml, $\Delta A_{290\ nm} = 0.00932$ per cm). The circular dichroism spectra are given as the difference in absorbance $\Delta A = A_L - A_R$.

The samples were prepared, under anhydrous conditions, by successive dilutions of the stock solution just before the spectra were recorded. Cuvette path lengths (0.2 to 100 mm) were calibrated with standard potassium chromate solutions in 0.05 N KOH. The concentrations of the monomer solutions ($CCl_4 + CH_3OH$) were calculated using the following extinction coefficients: $183 \cdot 10^3\ l \cdot mol^{-1} \cdot cm^{-1}$ (438 nm) and $26 \cdot 10^3\ l \cdot mol^{-1} \cdot cm^{-1}$ (625 nm) for PChl-a and $185 \cdot 10^3\ l \cdot mol^{-1} \cdot cm^{-1}$ (443

nm) and $21.9 \cdot 10^3$ l · mol^{-1} · cm^{-1} (628 nm) for VPChl-*a* in 0.5 % CH_3OH/CCl_4. These extinction coefficients were determined by comparison with the values in ether [9].

Preliminary ^{1}H NMR spectra were recorded using a Varian HA 100 spectrometer equipped with a data accumulation system. However, most of the spectra reported here were obtained with a Bruker XL-90 instrument, in pulse Fourier transform mode. The temperature was maintained at 25 °C. Varian microcells (120–150 µl) were used. The samples were prepared as for IR spectra by dissolving the pigment in dry C^2HCl_3 (99.9 %), and the concentration was determined by visible absorption after dilution with ether. All chemical shifts are given in δ, ppm, downfield from TMS added into the sample solutions. The titration with $C^2H_3O^2H$ (99.9 %) was carried out by adding successive portions of pure [U^2H]methanol with a precision microliter syringe. The integration of single peaks was carried out with a planimeter.

The absorption and CD spectra were decomposed with a Dupont curve resolver. Before being analyzed, the spectra were transformed to a linear energy scale. The absorption spectra were fitted to a linear combination of a minimum set of Gaussian functions (one for each transition in the case of monomer and two in the case of dimer) whose parameters (shape, position and amplitude) were changed so that their sum approximates the experimental spectrum. The half-width was 300 to 600 cm^{-1}, values generally encountered for the chlorophyll pigments [10]. The CD spectra were decomposed by the same method, trying to extract from the experimental spectrum, the double symmetric exciton signal which may be related to the geometry of the dimer. The same band width was used for CD and absorption bands.

Determination of dimerization constant

We used the method previously described for the study of dyes [34, 35] and chlorophylls [19].

The dimer association constant is defined as $K_D = C_D/C_M{}^2$ where C_D and C_M are respectively the molar concentration of dimer and monomer. The determination of the amounts of monomer and dimer was made at the wavelengths of the absorption maximum of the monomer: 626 nm and 438 nm for PChl-*a* and 626 nm and 443 nm for VPChl-*a*.

The total pigment concentration was determined by measuring the absorbance of the solution after disaggregation with methanol. The molar absorption coefficient of the pigment in 0.5 % methanol/CCl_4 was used as molar coefficient of the monomer. The extinction coefficient of the dimer was determined using a very concentrated solution ($5 \cdot 10^{-4}$ M). It was assumed that, at these concentrations, all the pigment was present in the dimer state. This assumption seemed to be reasonable since only weak absorbance changes were seen when the pigment concentration increased above 10^{-4} M.

RESULTS

Infrared spectra

We have measured the infrared spectra of concentrated solutions ($5 \cdot 10^{-2}$ to $5 \cdot 10^{-3}$ M) of PChl-*a* and VPChl-*a* in carbon tetrachloride and in several other nonpolar solvents (benzene, chloroform, cyclohexane). All spectra showed the

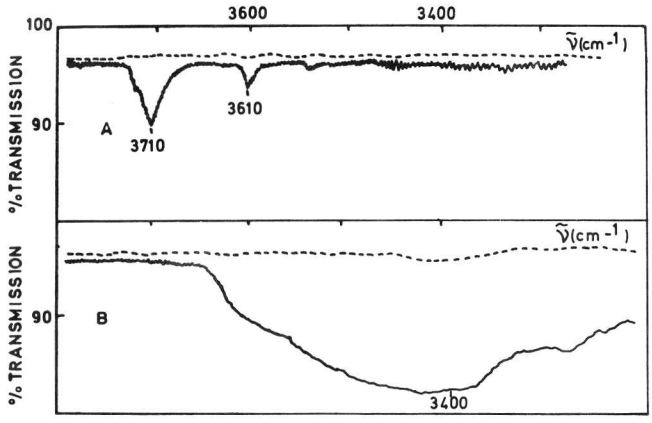

Fig. 1. Infrared spectra in the 3000–3800 cm^{-1} region (IRTRAN cell; 2 mm pathlength). (A) - - -, anhydrous CCl_4; —, water-saturated CCl_4; (B) - - -, anhydrous PChl-*a* ($3 \cdot 10^{-2}$ M) in dry CCl_4; —, hydrated PChl-*a* ($4.1 \cdot 10^{-2}$ M) in CCl_4,

"aggregated" ketone carbonyl band at 1668–1672 cm^{-1} in agreement with Houssier and Sauer [8]. Both the position and the intensity of the "aggregated" band varied slightly with the solvent. The intensity of this band appears to be strongly dependent upon the degree of purity and drying conditions of the samples.

The addition of Lewis bases (0.5 % methanol) produced the immediate disappearance of the 1668 cm^{-1} band and the corresponding increase of the intensity of the free keto absorption at 1703 cm^{-1}. Under some conditions (Rasquain, A., Houssier, C. and Sironval, C., to be published), the addition of water traces into the solution causes a disaggregation. We observed this effect especially in CCl_4, a solvent in which water is reasonably soluble.

Infrared spectra in the OH stretching region (3200–3800 cm^{-1}) provide a valuable test of the presence or absence of water in the samples. In order to observe the water region, concentrated solutions and long light paths (2 to 10 mm) are required. Fig. 1A shows the spectra of anhydrous CCl_4 (dashed line) and of CCl_4 with $5 \cdot 10^{-3}$ M water (continuous line) in this region. In water saturated CCl_4, the symmetric and antisymmetric OH stretching modes of H_2O are seen at 3710 and 3610 cm^{-1}. The spectra of PChl-*a* before and after intense drying (see methods) are given in Fig. 1B. The broad absorption band at 3400 cm^{-1} is due to the presence of bound water; it disappears completely after drying and dissolution in highly anhydrous CCl_4.

An estimate of the water content of a dry pigment solution can be made using the data of Ballschmitter et al. [23] and Rappaport [32]. It gives less than 10^{-4} M water for our dried samples. Thus the PChl : water ratio is at least 100 : 1 for concentrated solutions. The very low level of the water content is confirmed by the absence of the water band at 1.89 μm in the near infrared spectra [33]. The absence of this band for a 100 mm path length indicates a water concentration lower than 10^{-5} M.

Absorption and circular dichroism spectra

Fig. 2 shows the absorption and circular dichroism spectra of PChl-*a* in CCl_4 and VPChl-*a* in cyclohexane. Owing to the high values of the extinction coeffi-

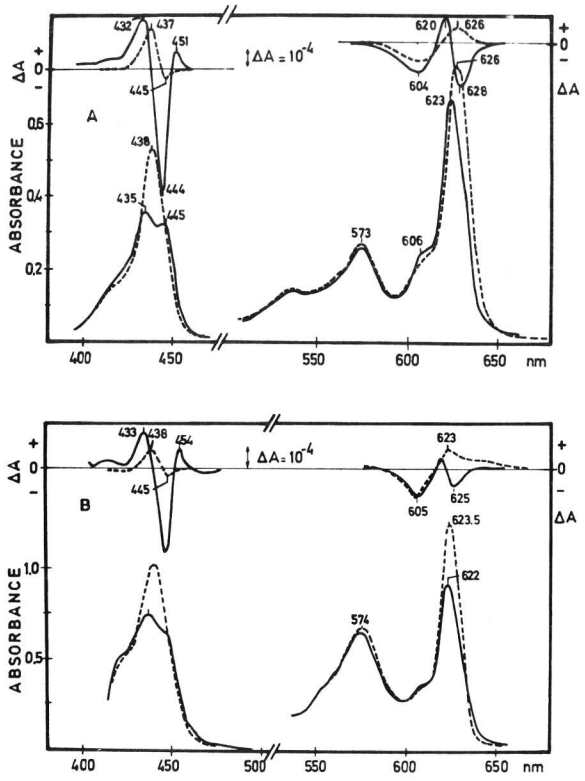

Fig. 2. (A) Absorption and circular dichroism spectra of anhydrous PChl-*a* ($1.8 \cdot 10^{-4}$ M) in dry CCl_4 (—) and in 0.5 % CH_3OH/CCl_4 (- - -). (Pathlengths: 0.2 mm for $\lambda < 500$ nm and 2 mm for $\lambda > 500$ nm.) (B) Absorption and circular dichroism spectra of anhydrous VPChl-*a* ($2 \cdot 10^{-5}$ M) in dry cyclohexane (—) and in 0.5 % methanol/cyclohexane (- - - -) (pathlengths: 5 mm for $\lambda < 500$ nm and 50 mm for $\lambda > 500$ nm).

cients, the pigment concentrations were less than 10^{-3} M. The spectra of PChl-*a* in dry CCl_4 (Fig. 2A) are in good agreement with those published by Houssier and Sauer (10). In dry CCl_4 (Fig. 2A, solid curves), the Q_Y absorption band at 623 nm shows a shoulder on the long wavelength side and a double CD characteristic of pigment-pigment interactions is observed for the principal transition in the red and in the blue regions. In the Soret region, the effects of the X and Y transitions add to each other and the two double CD bands of opposite sign appear as a triplet.

The addition of 0.5 % methanol results in a return to the monomer spectra (dashed curves in Fig. 2). The same behaviour was observed for the two pigments in all the nonpolar solvents used (CCl_4, C^2HCl_3, benzene, cyclohexane). The "aggregated" absorption and CD spectra of PChl-*a* and VPChl-*a* were found to be very sensitive to the presence of moisture in the solution. Intense drying of materials was required.

In carbon tetrachloride, the intensities of the principal absorption maxima decreased as the PChl-*a* (or VPChl-*a*) concentration increased. A monomer-dimer equilibrium in this solvent was clearly demonstrated by measuring the absorbance in

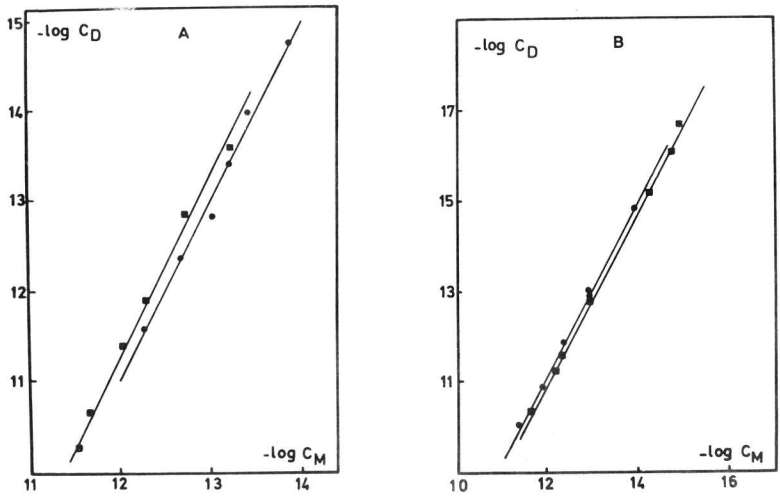

Fig. 3. (A) Log-log plot of dimer vs monomer concentration for PChl-*a* (●) and VPChl-*a* (■) in dry CCl_4. Absorbances measured in the red region; slope = 2 and $K_D = 7.4 \cdot 10^5$ l · M^{-1} for PChl-*a*; slope = 2.06 and $K_D = 5.5 \cdot 10^5$ l · M^{-1} for VPChl-*a*. (B) Log-log plot of dimer vs. monomer concentration for PChl-*a* (●) and VPChl-*a* (■) in dry CCl_4. Absorbances measured in the blue region; slope = 2.02 and $K_D = 4.2 \cdot 10^5$ l · M^{-1} for PChl-*a*; slope = 2.0 and $K_D = 5.5 \cdot 10^5$ for VPChl-*a*.

the red and in the blue bands for the $5 \cdot 10^{-4}$ to $5 \cdot 10^{-6}$ M pigment concentration range. Fig. 3 shows examples of log-log plots of the C_D versus C_M values obtained. The mean values for the dimerization constants in dry CCl_4 are $K_D = (6 \pm 2) \cdot 10^5$ l · mol^{-1} for PChl-*a* and $(4.5 \pm 2) \cdot 10^5$ l · m^{-1} for VPChl-*a* at 20 °C (averages of four series of measurements for each pigment). These values lead to standard free energies of dimer formation of −7.75 and −7.6 kcal · mol^{-1} respectively. The slope close to 2 is in full agreement with the hypothesis of a monomer-dimer equilibrium, and excludes the presence of greater aggregates.

^1H nuclear magnetic resonance spectra

Preliminary studies showed that the ^1H NMR spectra in nonpolar solvents are considerably different from those in polar solvents. They differ also from one nonpolar solvent to the other: well defined in C^2HCl_3, they are poorly resolved in cyclohexane. We have recorded ^1H NMR spectra of PChl pigments in C^2HCl_3 instead of CCl_4 in order to obtain a better resolution, but the conclusions are valid for both solvents.

Figs. 4 and 5 compare the spectra in C^2HCl_3 without (curves A) and with 0.5 % $C^2H_3O^2H$ (curves B). Most of the resonance peaks of the monomer (0.5 % $C^2H_3O^2H$ in C^2HCl_3) were assigned by considering the relative degree of deshielding due to the ring current of the macrocycle and by comparing them with the Chl-*a* spectrum. The chemical shifts are tabulated in Table I. It was not possible to assign unambiguously the methine proton (α, β, δ) resonances located at very low field (between 9 and 10 ppm). Nevertheless, because the α and β protons in VPChl-*a* are in nearly equivalent locations, they must give the peaks at 9.52 and 9.49 ppm. The third peak at 9.19 ppm for the VPChl-*a* and at 9.60 ppm for the PChl-*a*, is due to the δ proton resonance.

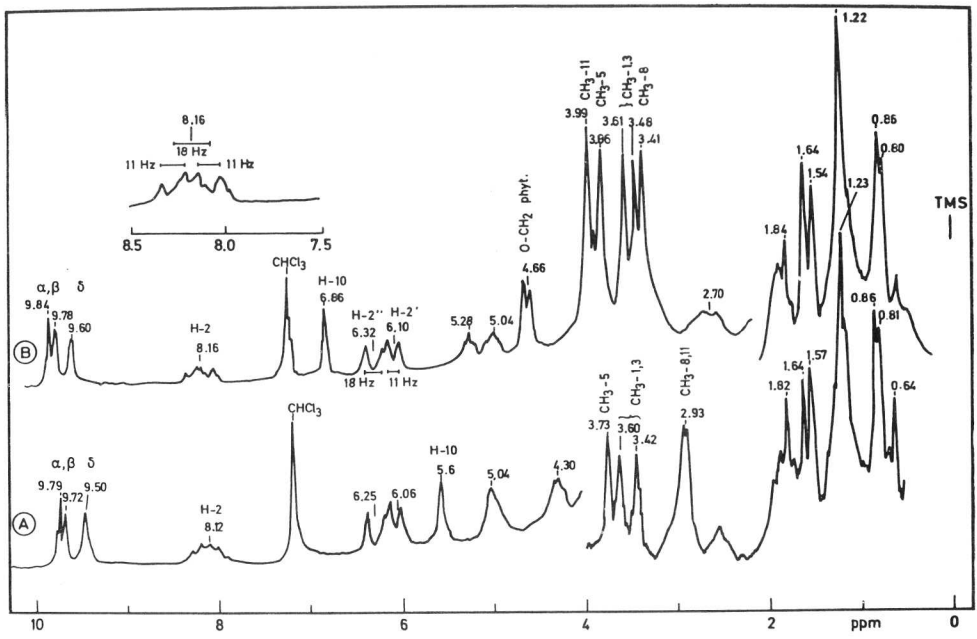

Fig. 4. ^{1}H magnetic resonance spectra at 100 MHz for anhydrous PChl-*a* ($3.5 \cdot 10^{-2}$ M) in dry C^2HCl_3 (curve A) and in 0.5 % $C^2H_3O^2H/C^2HCl_3$ (curve B).

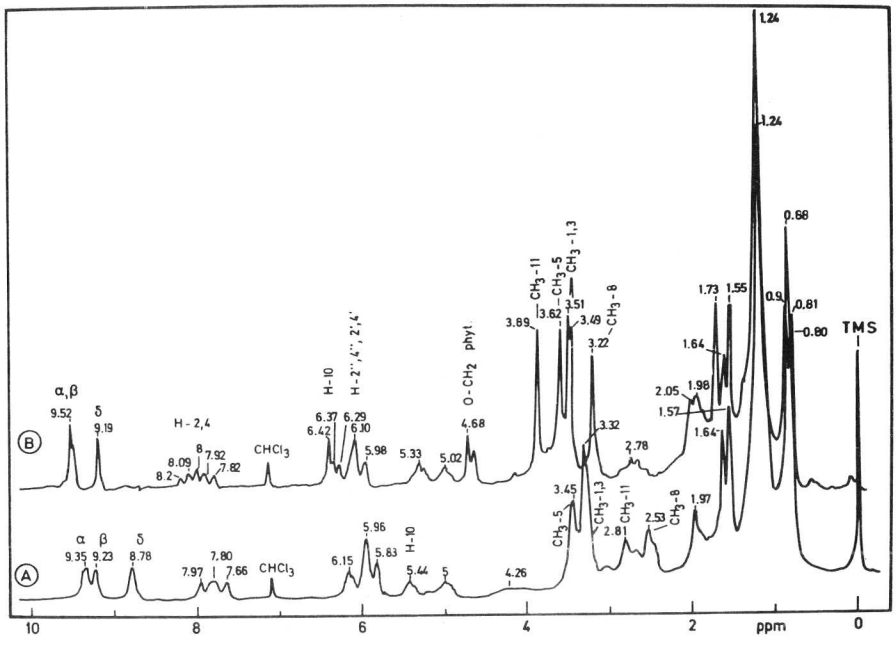

Fig. 5. ^{1}H magnetic resonance spectra at 90 MHz for anhydrous VPChl-*a* ($5 \cdot 10^{-2}$ M) in dry C^2HCl_3 (curve A) and in 0.5 % $C^2H_3O^2H/C^2HCl_3$ (curve B).

TABLE I

Chemical shifts (ppm from tetramethylsilane position) for protons of PChl-*a* and VPChl-*a* in C^2HCl_3 and 0.5 % $C^2H_3O^2H/C^2HCl_3$; $\Delta\delta$ is the difference between the chemical shifts of the monomer and the dimer. The protons numbering is indicated in Fig. 10.

Protons	PChl-*a*			VPChl-*a*		
	C^2HCl_3	$C^2H_3O^2H+C^2HCl_3$	$\Delta\delta$	C^2HCl_3	$C^2H_3O^2H+C^2HCl_3$	$\Delta\delta$
α, β	9.72 & 9.79	9.78 & 9.84	+0.06	9.35 & 9.23	9.49 & 9.52	+0.14 & +0.31
δ	9.50	9.60	+0.10	8.78	9.19	+0.41
2	8.12	8.16	+0.04	7.80	8 (H-2,4)	
2′	6.06	6.10	+0.04	centered	centered at	+0.20
2″	6.25	6.32	+0.07	at 6	6.20 (H-2″, 4″, 2′, 4′)	
10	5.6	6.86	+1.26	5.43	6.42	+0.99
11	2.93	3.99	+1.06	2.80	3.89	+1.09
5	3.73	3.86	+0.13	3.44	3.62	
CH_2-4	?	3.90	—	—	—	
1,3	3.60 & 3.42	3.61 & 3.48	+0.01 & 0.06	3.32 & 3.30	3.51 & 3.49	+0.19
8	2.93	3.41	+0.48	2.50	3.22	+0.72
7′						
7″					2.78 (?)	
Phytyl						
CH_2-		4.66	?	?	4.68	?
CH=	4.30	5.28	+1	4.26	5.33	+1

The vinyl group, in PChl-*a*, forms an AMX pattern. The coupling constants for $J_{2-2''}$ and $J_{2-2'}$ are respectively 19 Hz and 12 Hz; $J_{2'-2''}$ is not measurable. The distortion from a standard AMX pattern in VPChl-*a* may be explained by the occurence of two non-equivalent vinyl groups. The relative area of the AM part centered at 6.3 ppm is 5, instead of 4 as compared with a methine resonance. The supplementary absorbance at 6.42 ppm has the characteristics of the C-10 hydrogen. The resonance of this proton should be less affected by the ring current than the resonance of the methine protons; it should also be affected by the two adjacent carbonyl groups whose influence is however difficult to know exactly.

The comparison with the spectrum of Chl-*a* and the study of the disaggregation after alcohol addition allow us to assign the peaks at 6.86 ppm (PChl-*a*) and at 6.42 ppm (VPChl-*a*) to H-10. The doublet (J = 6 Hz) at 4.66 ppm for PChl-*a* (at 4.86 ppm for VPChl-*a*) with a relative area of 2 belongs to the two hydrogens of the first carbon of the phytyl chain. These protons are coupled to the olefinic proton which appears as a poorly resolved triplet at 5.28 ppm (5.33 ppm for VPChl-*a*).

The titration with $C^2H_3O^2H$ was of great help in deriving these assignments. The methyl group attached to the conjugated system (CH_3–1,3,5,8) and the acetyl carbonyl at position 10 (CH_3-11) form a set of five peaks at relatively low field between 3 and 4 ppm. These "low-field" methyl protons may be assigned with a reasonable degree of certainty by comparison with Chl-*a*. The CH_3-11 at the vicinity of the

ketone carbonyl is found at nearly the same field value as in Chl-a: 3.99 ppm and 3.89 ppm for PChl-*a* and VPChl-*a* respectively. The 1 and 3 methyl in VPChl-*a* exhibit nearly the same shielding: 3.51 and 3.49 ppm. They are better resolved in PChl-*a* spectrum: the peaks at 3.61 and 3.48 ppm are assigned to them, but they cannot be distinguished one from the other.

The peaks at 3.86 ppm in PChl-*a* and 3.62 ppm in VPChl-*a* are associated with the methyl hydrogens at position 5 in comparison with Chl-*a* [15]. The methyl at position 8 which gives a singlet at 1.73 ppm in Chl-*a* is located in the "low field methyl" region at 3.41 ppm and 3.22 ppm for PChl-*a* and VPChl-*a* respectively.

The resonances of the numerous protons of the phytyl chain complicate the "high field methyl" region below 2 ppm. Most of the signals were identified; they have chemical shift parameters which correspond closely to those of the free phytol. The methylene resonance of the group at position 4 in PChl-*a* is observed by the signals from the "low field methyls". The location of the resonances of the propionic acid CH_2 group (7′ and 7″) has not been established. A multiplet at 2.7 ppm may be due

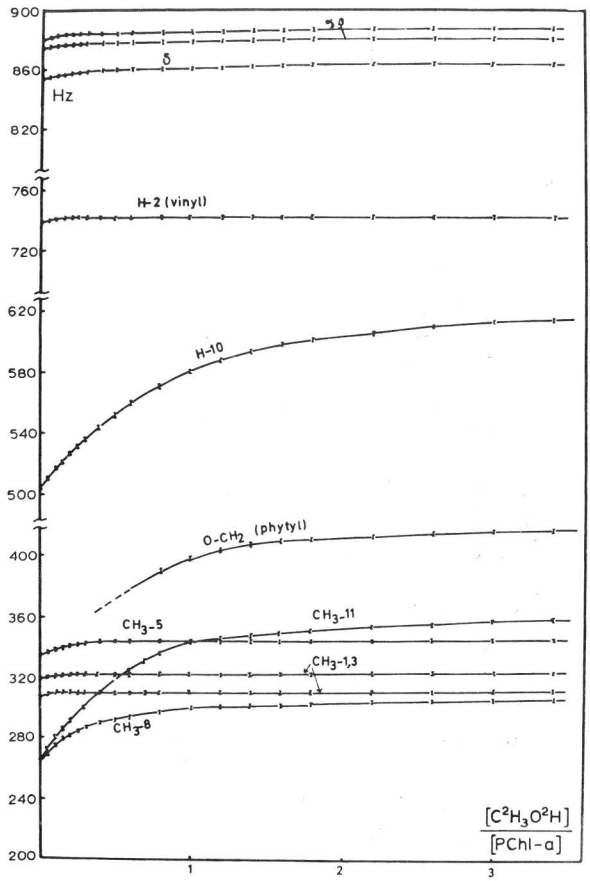

Fig. 6. Chemical shifts for ^1H magnetic resonance absorption of PChl-*a* ($3.5 \cdot 10^{-2}$ M) in C^2HCl_3 as a function of $C^2H_3O^2H$/pigment concentration; chemical shifts are downfield from tetramethylsilane.

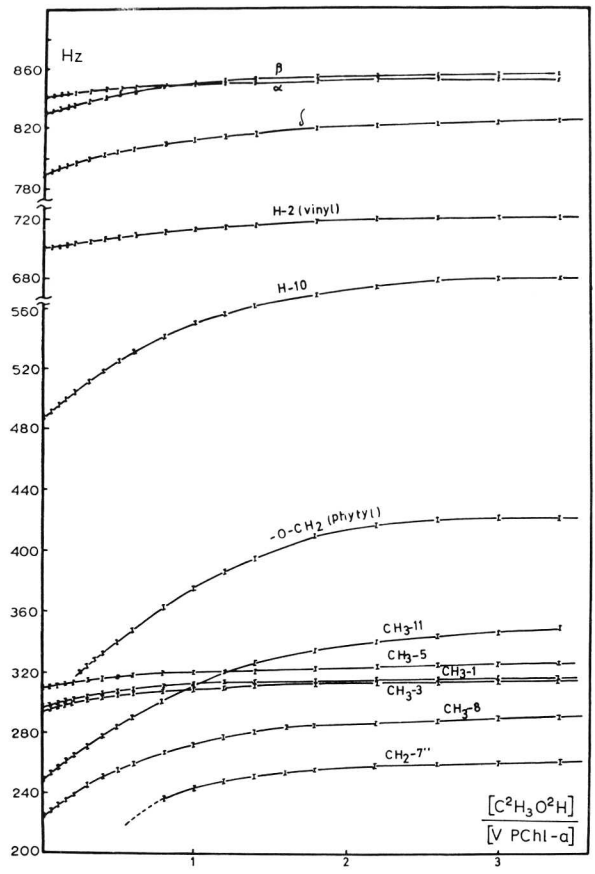

Fig. 7. Chemical shifts for ^1H magnetic resonance absorption of VPChl-*a* ($5 \cdot 10^{-2}$ M) in C^2HCl_3 as a function of $C^2H_3O^2H$/pigment concentration; chemical shifts are downfield from tetramethylsilane.

to one of these methylenes, the other being hidden among the phytyl resonances. Good agreement is generally observed with the assignment of Biere for a synthetic PChl-*a* [42]. A shift to higher field in the case of Biere's pigment may be due to differences in concentration or dryness.

In dry C^2HCl_3, the spectra are quite different from those obtained when methanol is added (compare Figs. 4 and 5 and see Table I). The addition of deuterated methanol was carried out as a titration. The chemical shift changes of the different hydrogens are shown in Figs. 6–7. They were plotted as a function of the methanol/pigment ratio. Minor changes occur in the position of the methine, vinyl and CH_3-1, 3,5 protons. However, large paramagnetic shifts are seen for the C-10, CH_3-8 and 11 protons and for the oxygen bonded methylene group of the phytyl chain. Except for the hydrogen on the first two carbons, the phytyl proton resonances are unaffected.

The spectra in dry C^2HCl_3 indicate the presence of interactions between pigment molecules. The upfield shift experienced by several protons in the nonpolar solvent has been explained by Closs et al. [15] in the case of Chl-*a* by the fact that a dimer is formed, in which one molecule is partially covered by the ring of another.

The addition of Lewis bases converts the dimer into a solvated monomer and the resonances move to lower field values.

NMR spectra of PChl pigments in dry C^2HCl_3 show very little concentration dependence. We recorded spectra in the $5 \cdot 10^{-2}$ M to $2.5 \cdot 10^{-3}$ M concentration range and the shifts were found to be very small for a dilution factor of 20. This is consistent with the high dimerization constant deduced from the behaviour of the visible absorption and CD spectra. This behaviour upon dilution in dry C^2HCl_3 indicates little structural change of the pigment arrangement over the concentration range studied. The same absence of significant dilution shift is observed in methanol-containing solvents. This is in agreement with the lack of association between molecules of solvated monomer.

DISCUSSION

The aggregation peak observed in the infrared spectra and the exciton splitting in the circular dichroism spectra indicate that PChl pigments aggregate in a similar way to chlorophylls. Nevertheless, the analysis of visible and NMR spectra suggests a significantly different dimer structure from that of chlorophyll *a* and *b* and bacteriochlorophyll *a*. We shall discuss this point in more detail.

In dry CCl_4, the behaviour of PChl-*a* may be described as a monomer-dimer equilibrium:

$$2\ \mathrm{PChl} \overset{K_D}{\rightleftharpoons} \mathrm{PChl}_2.$$

The high dimerization constant (of the order of $5 \cdot 10^5\ l \cdot M^{-1}$) allows us to conclude that PChl-*a* and VPChl-*a* in concentrated solution in CCl_4 and probably also in C^2HCl_3 exist essentially in a dimeric form. This conclusion is in agreement with the fact that the free ketone peak is always visible in dry CCl_4 and C^2HCl_3: only one half of the ketone groups are involved in the dimer. Ballschmitter et al. [21] showed that Chl-*a* in CCl_4, even in solutions as concentrated as 0.1 M, is predominantly in a dimeric form. In cycloaliphatic solvents, however, oligomers are present at chlorophyll concentrations larger than 10^{-3} M. Such oligomers of PChl-*a* could also be present in dry cyclohexane, in which the pigment is less soluble.

From all of our spectral studies (IR, NMR, *A* and CD), it appears that dimers of PChl-*a* and VPChl-*a* in dry nonpolar solvents have very similar structures. All of the conclusions obtained from the study of one pigment will thus be applicable to the other.

Structure of dimer

A quantitative treatment of the absorption and circular dichroism spectra was made in order to collect information about the structure of the dimer. This analysis was usefully supplemented by that of the NMR data.

Absorption and circular dichroism. We used the theoretical model based on the point dipole interaction [36]; it constitutes a great oversimplification for molecules such as PChl-*a* but it is nevertheless useful and may give the relative orientation of the dipole transition moments of the associated molecules.

The parameters deduced from the decomposition of the red absorption spec-

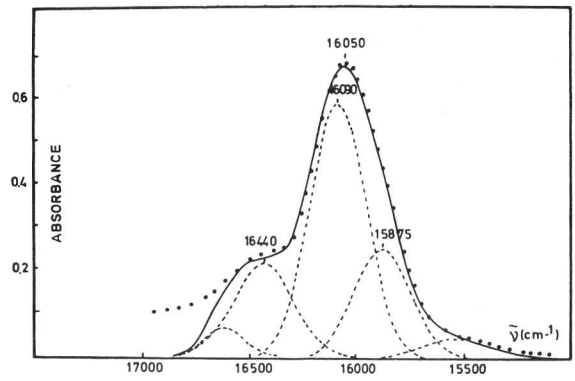

Fig. 8. Decomposition of the absorption spectrum (red bands) of PChl-*a* dimer into Gaussian components (dashed curves). The sum of the Gaussian components (—) is compared to experimental data (. . .). The derived parameters are summarized in Table II.

TABLE II

SPECTRAL PARAMETERS RELATIVE TO THE ABSORPTION AND CIRCULAR DICHROISM SPECTRA OF PChl-*a* IN THE RED REGION

	Q_X transition	Q_Y transition		
Monomer (absorption)				
λ_{max}, nm	608		626	
$\tilde{\nu}_{max}$, cm^{-1}	16 430		15 990	
$\Delta\tilde{\nu}_{\frac{1}{2}}$, cm^{-1}	400		400	
D, debye^2	1.47		6.35	
Dimer (absorption)		Component 1		Component 2
λ_{max}, nm	608	621.5		630
$\tilde{\nu}_{max}$, cm^{-1}	16 440	16 090		15 875
$\frac{\tilde{\nu}_+ + \tilde{\nu}_-}{2}$, cm^{-1}			15 982	
$\tilde{\nu}_+ - \nu_-$, cm^{-1}			$\pm$215	
$\Delta\tilde{\nu}_{\frac{1}{2}}$, cm^{-1}	325	325		325
$D_\pm$, debye^2		8		3,42
$\frac{D_+ + D_-}{2}$, debye^2			5.7	
D_+/D_-			2.34 or 0.43	
θ_{12}, deg.			66 or 114°	
Dimer (circular dichroism)				
$\tilde{\nu}_{max}$, cm^{-1}	15 570	16 100		15 900
$\frac{\tilde{\nu}_+ + \tilde{\nu}_-}{2}$, cm^{-1}			15 990	
$\tilde{\nu}_+ - \tilde{\nu}_-$, cm^{-1}			$\pm$185	
ΔA	$-1.4 \cdot 10^{-4}$	$+2.8 \cdot 10^{-4}$		$-2.8 \cdot 10^{-4}$
$\Delta\tilde{\nu}_{\frac{1}{2}}$, cm^{-1}	325	325		325
$R_\pm$, debye-magneton		+0.103		−0.103

trum of the monomer in 0.5% methanol/carbon tetrachloride using Gaussian functions are reported in Table II. Each main transition (Q_Y and Q_X) is represented by one Gauss of 400–450 cm^{-1} half-width. We have performed a quantitative treatment of the absorption data in the red region, for the dimer of PChl-*a*, trying to assign a half-width parameter of the same order of magnitude as for the monomer bands. Fig. 8 shows the decomposition of the red absorption band of $4 \cdot 10^{-4}$ M solution of PChl-*a* in dry CCl_4. At this high concentration we may consider that nearly all the pigment is aggregated. The calculated absorption spectrum fits the experimental spectrum satisfactorily if two Gauss of 325 cm^{-1} half-width are chosen for the Q_Y band (15875 cm^{-1} and 16090 cm^{-1}) and one main Gaussian function (16440 cm^{-1}) for the Q_X. The position of the two components of the Q_Y transition is not clearly visible in the absorption spectrum. A very weak shoulder appears on the long-wavelength side. The derivative spectrum shows more clearly its position near 15850 cm^{-1}. One of the components being fixed at this position, the suggested decomposition may be considered as unique.

No splitting was visible for the small Q_X band at 16440 cm^{-1}. It can be represented by a unique Gaussian function. Supplementary Gauss must be added at each side of the spectrum to obtain a better fitting. These additional bands don't have any influence in the further analysis.

The spectral parameters relative to the absorption spectrum of the dimer are presented in Table II. The formula giving the dimer dipole strengths may be expressed as [37]:

$$\frac{D_+}{D_-} = \frac{1+\cos\theta_{12}}{1-\cos\theta_{12}}$$

where θ_{12} is the intertransition moment angle. With $D_+/D_- = 2.34$ or 0.43 (since the in-phase and out-of-phase components cannot be assigned from the experiments) we obtained an angle of 66° or 114° for the Q_Y transition moments of the two molecules in the dimer.

The CD spectrum introduces a somewhat different problem. As generally observed for other compounds, the double CD signal of PChl dimers is not symmetrical. In practice, the degenerate exciton interaction must be extracted from the experimental spectrum to be related to the detailed geometry of the dimer, using the equations of Tinoco [37].

The deconvolution of the experimental CD spectrum of PChl-*a* dimer in dry CCl_4 has been carried out using the exciton component positions and half-widths derived from the absorption spectrum (Fig. 9). The best fitting has been obtained by introducing, in addition to two exciton components for the Q_Y band (15900 and 16100 cm^{-1}) a weak negative Gaussian at 16025 cm^{-1} to represent the non-degenerate component. The sum of the two exciton components of equal amplitude (15900 and 16100 cm^{-1}) gives a signal which passes through zero near the absorption maximum of the monomer at 16020 cm^{-1} (see Fig. 9B). As in absorption, the Q_X band is fitted by a unique Gaussian band of negative sign in this case (16570 cm^{-1}). If the monomer contribution to the dimer CD spectrum is subtracted before decomposition, the exciton parameters deduced are not significantly different.

The parameters (rotational strengths, exciton splitting) deduced from the CD

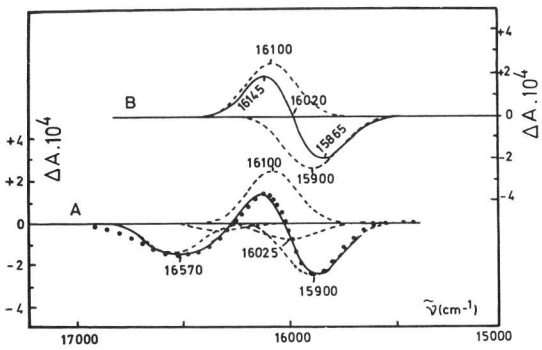

Fig. 9. (A) Decomposition of the circular dichroism spectrum (red bands) of PChl-*a* dimer into Gaussian components (dashed curves). The sum of the Gaussian components (—) is compared to experimental data (. . .). (B) Degenerated exciton interaction extracted form the experimental spectra. The derived parameters are summarized in Table II.

spectra analysis (Table II) may be compared with the values calculated on the basis of particular geometrical models. Two models of dimer structure have been considered, the first one involving a parallel stacking and the second one a perpendicular arrangement of the associated molecules. In the two cases, the monomer molecules are linked together by C = O - - - Mg interaction.

For parallel planes (Fig. 11A) the dissymmetry factor is:

$$\frac{R_{\pm}}{\tilde{\nu}_0 \mu^2} = \mp \frac{\pi}{2} \cdot d \sin \theta_{12}$$

where d is the distance between the planes (with a minimum acceptable value of 3.5 Å) and θ_{12} the intertransition moment angle for the Q_Y transition. The experimental $|R_{\pm}|$ value introduced in this formula yielded an intertransition moment angle for Q_Y:

$$\theta_{12} = 11^\circ \text{ or } 160^\circ$$

The value for the exciton splitting is:

$$\Delta\tilde{\nu}_Y = \frac{2\mu^2}{hCR_{12}^3} [\cos \theta_{12} - \tfrac{3}{2} \cos^2 27^\circ (\cos \theta_{12} + \cos (2\beta - \theta_{12})]$$

where $\beta = 25^\circ$.

The exciton splitting is found to be negative for $\theta_{12} = 11^\circ$; this is in agreement with the CD spectrum of PChl-*a* in which the negative component appears at longer wavelength. The value of θ_{12} deduced from absorption and CD spectra is in complete disagreement. Such a large discrepancy cannot be attributed to the inadequacy of the point dipole model and is taken as an argument against the parallelism of the porphyrin planes.

Fong [39] proposed a symmetrical dimer structure for $(\text{Chl-}a)_2$ involving two reciprocal C-10 ester CO - - - Mg interactions between parallel chlorophyll molecules. This model is in complete disagreement with the fact that pyrochlorophyll *a* which does not have the ring V carbomethoxy group aggregates in a similar way to Chl-*a* and

shows the aggregated ketone band at 1650 cm^{-1} [22]. It seems thus evident that the C-10 carbomethoxy group is not involved in dimer formation and that the porphyrin rings do not lie in parallel planes.

The second model assumes a perpendicular arrangement for the two molecules in the dimer (Fig. 11B). The dissymmetry factor is:

$$\frac{R_{\pm}}{\tilde{\nu}_0 \mu^2} = \mp \frac{\pi}{2} R_{12} \sin 20^\circ \cos \Phi$$

$$\cos \theta_{12} = \sin \Phi \sin 10^\circ$$

When molecule 1 turns around the C = O - - - Mg axis ($0^\circ \leqslant \Phi \leqslant 180^\circ$), the dissymmetry factor of the (+) band varies from $-4.27 \cdot 10^{-8}$ cm ($\Phi = 0^\circ$) to $+4.27 \cdot 10^{-8}$ cm ($\Phi = 180^\circ$), cancelling for $\Phi = 90^\circ$. The experimental value for the Q_Y transition of PChl-*a* ($1 \cdot 10^{-8}$ cm) yields $\Phi = 75^\circ$ or 105° and $\theta_{12} = 80^\circ$; this value of intertransition moment angle (80°) deduced from CD spectra is in better agreement with that deduced from absorption spectra (66°), than in the case of the parallel arrangement.

The exciton splitting for the Y transition is

$$\Delta\tilde{\nu} = \frac{2\mu^2}{hcR_{12}^3} \cos \theta_{12}(1 - 3 \cos 20^\circ)$$

For a value of $\Phi = 75^\circ$, $\Delta\tilde{\nu}$ is negative. The $\tilde{\nu}_+$ component must be of lower energy and the rotational strength is negative since cos Φ is positive. This is in agreement with the PChl dimer spectra in which the longest wavelength CD component is negative. For an angle of 105°, the $\tilde{\nu}_+$ component of the CD spectrum is located at longer wavelength; this is the case of Chl-*a*. Identical conclusions were obtained with Φ angle values of 255° and 285°. For the two Φ angle values (75° or 105°) the plane of molecule 2 (see Fig. 11B) is situated at each side of the Y axis of molecule 1. Thus, it appears that a weak difference in structural arrangement of the two associated molecules can explain the reversal of sign of the PChl CD spectra in comparison with that of the Chl spectra.

The perpendicular arrangement is that proposed by Shipman et al. [40] for Chl dimers and it appears more satisfying than the parallel stacking since it optimizes the directionality of the C = O - - - Mg bond and minimizes steric repulsions between the two porphyrin rings [40]. In the present analysis, we have not considered environmental effects as in the treatment of Shipman et al. As far as we know the influence of these effects on the rotational strength has not been theoretically examined.

Other arrangements involving interplanar angles between 0° and 90° are also conceivable and could probably yield a satisfactory fitting of the experimental spectra. The determination of the exact geometry of the dimer with intermediate interplanar angle requires the determination of the interaction parameters in two differently oriented transitions. In the case of bacteriochlorophyll *a*, the Q_X and Q_Y transitions are well separated and this allowed Dratz [41] to deduce the dimer structure for such a configuration. The Q_X transition of PChl *a*, however, showing no evidence of splitting, the B_X transition must be considered. Unfortunately, the blue region is a composite of two nearly degenerate transitions ($\Delta\tilde{\nu}$ is 360 cm^{-1} in the monomer) which are both

split into two components when the dimer is formed. The decomposition of the absorption and CD spectra in the Soret region was found very difficult and did not yield unambiguous answers.

If we consider the transitions polarized along the x axis, we see that the B_X transition displays an exciton splitting while the Q_X transition doesn't. Undoubtedly, the Q_X splitting is the most difficult to observe because it is the weakest transition and it lies beneath vibronic components of the intense Q_Y transition. Furthermore, PChl-*a* which has nearly D_{4h} symmetry, may be the molecule for which the point dipole approximation is least applicable. We believe, however, that this observation results from the fact that the strong B_X transition is not oriented exactly in the same direction as the weak Q_X transition. Lhoste [38] suggested that in the most symmetric porphyrins, the transitions are not rigorously polarized along parallel or perpendicular directions. Owing to these numerous difficulties, we are not able to further analyse our CD and absorption data.

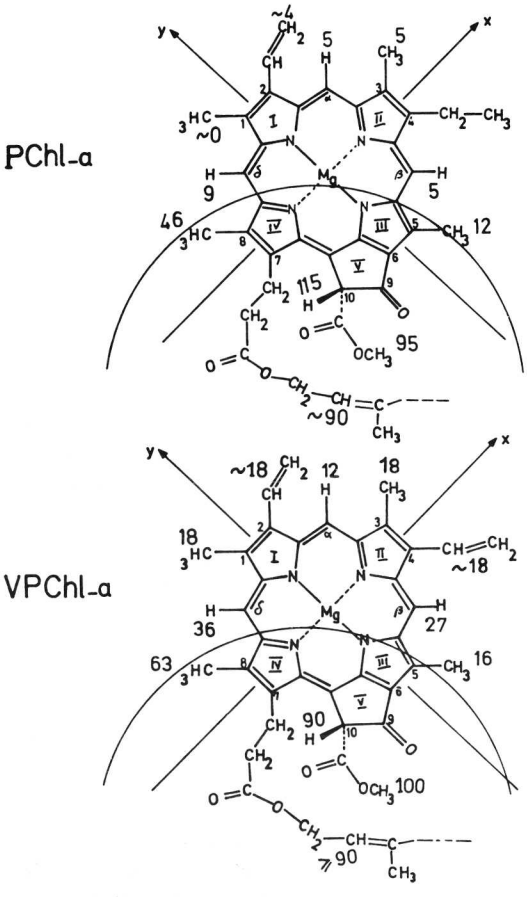

Fig. 10. Aggregation maps of PChl-*a* and VPChl-*a*. The shift differences (in Hz) between dimer (C^2HCl_3) and monomer (0.5 % $C^2H_3O^2H/C^2HCl_3$) are indicated for the individual protons. The semi-circle indicates the area of maximum interaction in the dimer.

NMR data analysis. The shifts observed in the NMR spectra of PChl pigments in chloroform solutions must be attributed to the presence of specific interactions among the pigment molecules. The close examination of the ring current effect on the different hydrogens can be used to provide a detailed picture of the nature of pigment-pigment interactions.

It can be seen from Figs. 6 and 7 that not all of the protons are equally involved in the aggregation process. The protons of rings IV and V (H-10, CH_3-8 and 11, CH_2-phytyl) are the most subjected to strong shielding by the associated molecule while the protons of rings I and II are practically unaffected. This means that the dimer is asymmetric and that only a part of the ring of one molecule is eclipsed by the other. The titration data of Figs. 6 and 7 can be presented in the form of an aggregation map (Fig. 10). The maximum shift differences are indicated for the individual protons.

The semi-circle represents the influence of the second monomer unit; the region of ring overlap is clearly defined to occur near ring V. This observation is consistent with the existence of a C = O - - - Mg interaction and with the structural model proposed from electronic spectra analysis. In the perpendicular arrangement (Fig. 11B), for a value of $\Phi = 75°$, the regions of ring V are in front of each other. An interplanar angle lower than 90° may tend to put the regions of rings III, IV and V of the two molecules in closer proximity.

The chemical shift observed for the protons of methyl-8 is larger than for

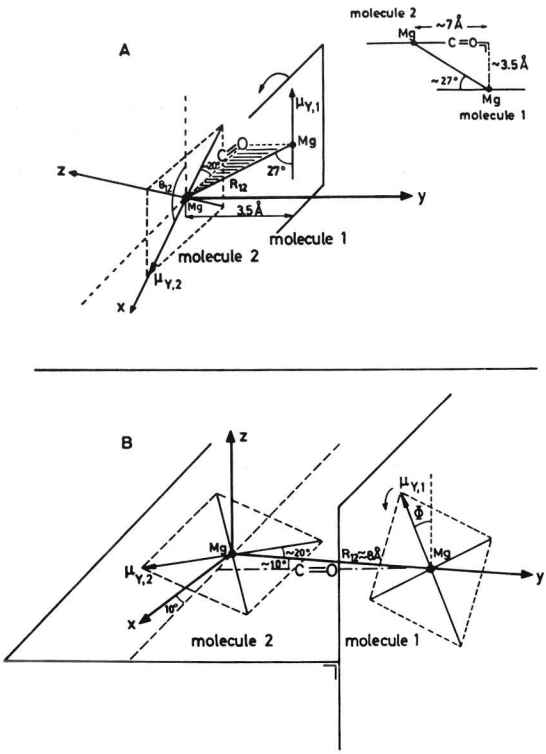

Fig. 11. Two PChl dimer structures; A, parallel arrangement; B, perpendicular arrangement. θ_{12} is the intertransition moment angle (Q_Y transition).

methyl-5, contrary to the case of Chl-*a*; this suggests that the interaction must be stronger in the vicinity of ring IV in the PChl-*a* dimer. This interesting observation must be related to the difference in the sign of the CD components of PChl-*a* compared to Chl-a and attributed to a significantly different structure for the porphyrin and dihydroporphyrin dimers. The fact that C_7-C_8 bond is not reduced in the porphyrins is probably favourable for a better overlapping in this region.

The fact that protons of rings I and II are unaffected is an indication that no further aggregation to higher polymer seems to occur even at the highest concentrations. The orientation of one chromophore with respect to the other is such that all the protons are not equivalent in the two associated molecules. However, only one set of lines is observed in the NMR spectra. The dynamic equilibrium between two monomer units must be rapid: each molecule is alternatively donor or acceptor. All the ^1H NMR data are consistent with infrared and visible observations and are compatible with dimer formation in C^2HCl_3 and CCl_4 solutions.

On the basis of all spectral properties examined in this paper, we conclude that PChl pigments in dry nonpolar solvents tend to form predominantly a dimer. The porphyrin planes of associated chromophores could be perpendicular to one another. This structural arrangement is in agreement with (i) the optimal directionality for the C = O - - - Mg bond, (ii) the comparison of absorption and circular dichroism parameters, (iii) the upfield shift observed in NMR spectra. It may constitute a model for the state of the pigment in vivo.

ACKNOWLEDGMENTS

This work was supported by grants from "l'Institut pour l'Encouragement de la Recherche Scientifique dans l'Industrie et l'Agriculture", le Patrimoine de l'Université de Liège et le Fonds de la Recherche Fondamentale Collective (Belgium). The authors are very grateful to Dr. J. Denoel for recording NMR spectra and to Professor K. Sauer for helpful comments and suggestions.

REFERENCES

1 Butler, W. L. and Briggs, W. R. (1966) Biochim. Biophys. Acta 112, 45–53
2 Dujardin, E. and Sironval, C. (1970) Photosynthetica 4, 129–138
3 Sironval, C. (1972) Photosynthetica 6, 375–380
4 Kahn, A., Boardman, N. K. and Thorne, S. W. (1970) J. Mol. Biol. 48, 85–101
5 Schultz, A. and Sauer, K. (1972) Biochim. Biophys. Acta 267, 320–340
6 Mathis, P. and Sauer, K. (1972) Biochim. Biophys. Acta 267, 498–511
7 Schopfer, P. and Siegelman, H. W. (1968) Plant Physiol. 43, 990–996
8 Houssier, C. and Sauer, K. (1969) Biochim. Biophys. Acta 172, 476–491
9 Houssier, C. and Sauer, K. (1969) Biochim. Biophys. Acta 172, 492–502
10 Houssier, C. and Sauer, K. (1970) J. Am. Chem. Soc. 92, 779–791
11 Seliskar, C. J. and Ke, B. (1968) Biochim. Biophys. Acta 153, 685–691
12 Brouers, M. (1972) Photosynthetica 6, 415–423
13 Katz, J. J., Closs, G. L., Pennington, F. C., Thomas, M. R. and Strain, H. H. (1963) J. Am. Chem. Soc. 85, 3801–3809
14 Anderson, A. F. H. and Calvin, M. (1964) Arch. Biochem. Biophys. 107, 251–259
15 Closs, G. L., Katz, J. J., Pennington, F. C., Thomas, M. R. and Strain, H. H. (1963) J. Am. Chem. Soc. 85, 3809–3821
16 Katz, J. J. (1973) Inorganic Biochemistry (Eichorn, G. I., ed.), pp. 1022–1066 Elsevier, Holland

17 Katz, J. J., Strain, H. H., Leussing, D. L. and Dougherty, R. C. (1968) J. Am. Chem. Soc. 90, 784–791
18 Katz, J. J., Janson, T. R., Kostka, A. G., Uphaus, R. A. and Closs, G. L. (1972) J. Am. Chem. Soc. 94, 2883–2885
19 Sauer, K., Smith, J. R. L. and Schultz, A. J. (1966) J. Am. Chem. Soc. 88, 2681–2688
20 Dratz, E. A., Schultz, A. J. and Sauer, K. (1966) Brookhaven Symp. Biol. 19, 303–318
21 Ballschmitter, K., Truesdell, K. and Katz, J. J. (1969) Biochim. Biophys. Acta 184, 604–613
22 Ballschmitter, K. and Katz, J. J. (1969) J. Am. Chem. Soc. 91, 2661–2667
23 Ballschmitter, K., Cotton, J. M., Strain, H. H. and Katz, J. J. (1969) Biochim. Biophys. Acta, 180, 347–359
24 Sherman, G. and Wang, S. F. (1967) Photochem. Photobiol. 6, 239–245
25 Ballschmitter, K. and Katz, J. J. (1972) Biochim. Biophys. Acta 256, 307–327
26 Sherman, G. and Linschitz, H. (1967) Nature 215, 511
27 Sherman, G. and Wang, S. F. (1966) Nature 212, 588–590
28 Katz, J. J. and Norris, J. R. (1973) Current Topics in Bioenergetics (Sandi, D. R. and Packer, L., eds.), Vol. 5, pp. 41–75, Academic Press, New York
29 Trifunac, A. D. and Katz, J. J. (1974) J. Am. Chem. Soc. 96, 5233–5240
30 Cotton, T. M., Trifunac, A. D., Ballschmitter, K. and Katz, J. J. (1974) Biochim. Biophys. Acta 368, 181–198
31 Boxer, S. G., Closs, G. L. and Katz, J. J. (1974) J. Am. Chem. Soc. 96, 7058–7066
32 Rappaport, G. (1966) Thesis Ohio State University, No. 67–2518 University Microfilms, Ann. Arbor, Mich
33 Stevenson, D. P. (1965) J. Phys. Chem. 69, 2145–2152
34 West, W. and Pearce, S. (1965) J. Phys. Chem. 69, 1894–1903
35 Bergmann, K. and O'konski, C. T. (1963) J. Chem. Phys. 67, 2169–2177
36 Tinoco, Jr. I. (1963) Rad. Res. 20, 133–139
37 Tinoco, Jr. I. and Cantor, C. R. (1970) Methods of Biochemical Analysis (Glick, D., ed.), Vol. 18, pp. 81–203, Interscience Publishers, New York
38 Lhoste, J. M. (1968) Bull. Soc. Franç. Physiol. Végét. 14, 379–408
39 Fong, F. K. and Koester, V. J. (1975) J. Am. Chem. Soc. 97, 6888–6890
40 Shipman, L. L., Cotton, T. M., Norris, J. R. and Katz, J. J. (1976) J. Am. Chem. Soc. 98, 8222–8230
41 Dratz, E. A. (1966) Thesis, Berkeley University, California.
42 Biere, H. (1966) Thesis, Braunschweig, Germany